

Learning a Discriminative Prior for Blind Image Deblurring Supplemental Material

Lerenhan Li^{1,2} Jinshan Pan³ Wei-Sheng Lai² Changxin Gao¹
Nong Sang^{1*} Ming-Hsuan Yang²

¹National Key Laboratory of Science and Technology on Multispectral Information Processing,
School of Automation, Huazhong University of Science and Technology

²Electrical Engineering and Computer Science, University of California, Merced

³School of Computer Science and Engineering, Nanjing University of Science and Technology

Overview

In this supplemental material, we provide additional analysis on the robustness of the classifier to different blur degree, and discuss the robustness of the proposed deblurring method to noise. Then, we quantitatively evaluate our algorithm on the publicly available benchmark datasets [4, 12, 6] against state-of-the-art methods. Finally, we show more visual comparisons with state-of-the-art methods.

1. Main steps for optimizing (4) in the manuscript

We summarize the main steps for optimizing (4) in the manuscript in Algorithm 1.

Algorithm 1 Blur Kernel Estimation

Input: Blurred Image B

Output: Intermediate latent image I and blur kernel k .

```
1: initialize  $k$  with results from the coarser level
2: while  $i < \text{iter}_{\max}$  do
3:   solve for  $I$  by (7) in the manuscript.
4:   solve for  $k$  by (13) in the manuscript.
5:    $i \leftarrow i + 1$ 
6: end while
```

2. Further Analysis on the Proposed Algorithm

In this section, we analyze the robustness of the classifier to different blur degree, and discuss the robustness to noise of the proposed deblurring method.

2.1. Robustness to blur degree

As the discriminative prior is a binary classifier which is used to classify the blurred images and clear images, a natural question is that whether the discriminative prior is robust to blur degree (i.e., blur kernel size) or not. Here we further analyze the robustness of the proposed prior with different size of blur kernels. We synthesize 240 blur kernels with the size ranging from 5×5 to 51×51 (we generate 10 kernels for each size). Then we evaluate the accuracy of the binary classifier on an image with the size of 800×800 . Figure 1 shows that the proposed discriminative prior is robust to the blur degree with a wide range of the blur kernel size.

*Corresponding author.

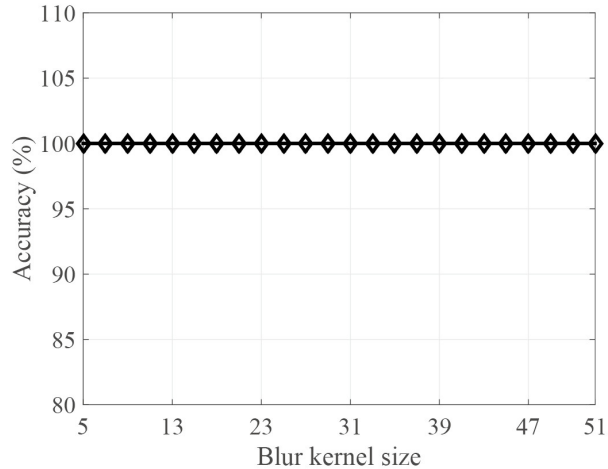


Figure 1. Classification accuracy on different blur kernel sizes. The classifier is robust to the blur degree with a wide range of the blur kernel size.

2.2. Robustness to noise

We analyze the influence of the Gaussian noise and salt and pepper noise on the proposed deblurring algorithm.

Gaussian noise: Figure 2 compares the deblurred results with state-of-the-art methods [10, 16] on an example which contains Gaussian noise. As the dark channel [10] and extreme channels priors [16] are based on pixel intensity, their performance is degraded by the noise in input images. In contrast, we use blurred images with 1% Gaussian noise when training our discriminative prior. The proposed method is more robust to Gaussian noise. However, when the noise level is larger, our image prior becomes less effective as shown in Figure 3. A straightforward solution to handle such noisy input images is to first apply a Gaussian filter to the blurred images before using our method for estimating the blur kernel. We show in Figure 3(c) that such approach can handle noisy blurred images to a certain extent.

To quantitatively evaluate the robustness of the proposed algorithm to Gaussian noise, we add the Gaussian noise with different noise levels from 1% to 5% on five blurred images. For fair comparisons, we use the same non-blind deconvolution method [17] to generate the final deblurred results. Figure 4(a) shows that the proposed method performs favorably against the state-of-the-art methods [10, 16] on different noise levels.

Salt and pepper noise: The proposed method is less robust to salt and pepper noise as the classification network cannot differentiate the blurred image with salt and pepper noise ($f(B) \simeq 0$). To further examine the sensitivity of our method, we test 5 blurred images with salt and pepper noise with the noise density ranging from 1% to 5%. Figure 4(b) shows that both the state-of-the-art methods [10, 16] and the proposed method do not perform well when the blurred images contain salt and pepper noise.



Figure 2. A blurred image with Gaussian noise. The image priors based on intensity information [10, 16] is less robust to images with Gaussian noise. In contrast, the deblurred results from the proposed algorithm have fewer artifacts as shown in the zoom-in areas.

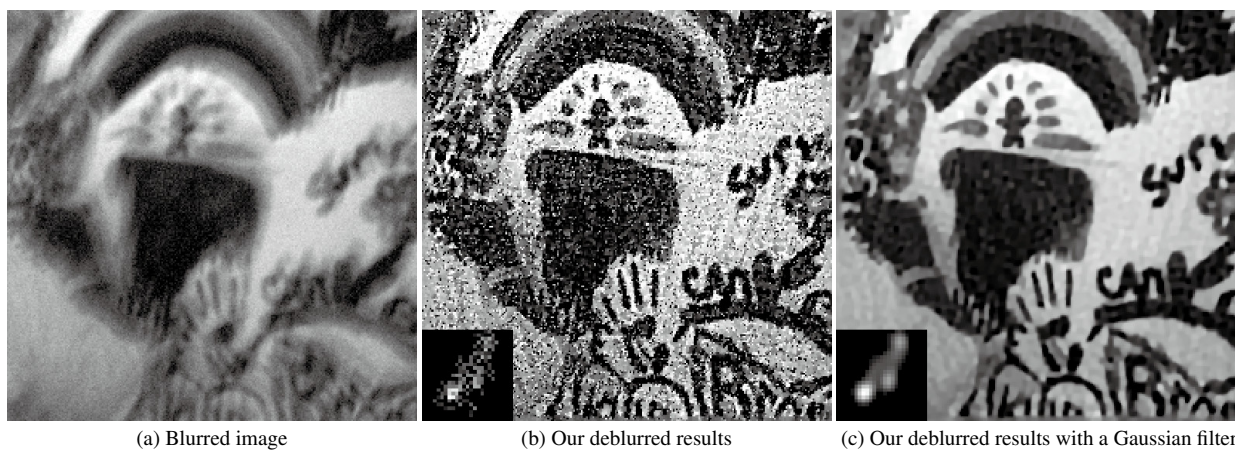


Figure 3. An example with severe Gaussian noise. Our algorithm does not work well as the learned image prior cannot differentiate blurred and clear image under such cases. We first apply a Gaussian filter and then adopt our method for deblurring to handle inputs with severe Gaussian noise.

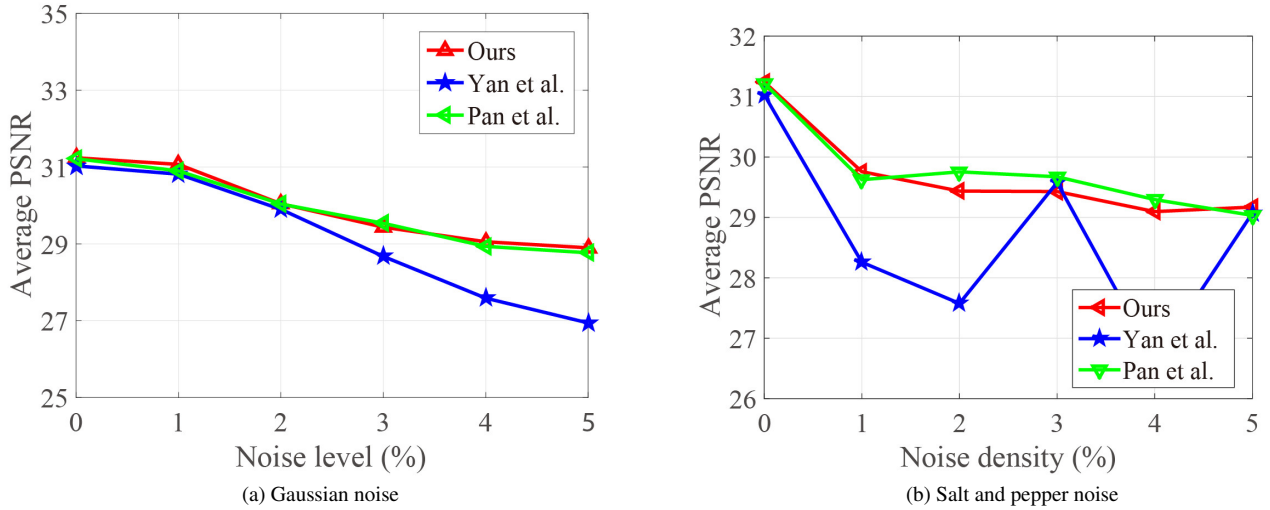


Figure 4. Evaluations on the blurred images with noise. Our method performs favorably against state-of-the-art methods [10, 16] on handling Gaussian noise. However, both state-of-the-art approaches [10, 16] and our method are less effective when images contain salt and pepper noise.

3. Quantitative Evaluations on Available Deblurring Datasets

To verify the effectiveness of our method, we further evaluate it on deblurring benchmarks [4, 12, 6]. Figure 5 shows the comparisons with state-of-the-art methods on the datasets [4, 12]. Figure 6 (a) shows that our method generates competitive results with state-of-the-art methods. In particular, it achieves 100% success rate at error ratio 2. These three examples whose error ratios are higher than 1.5 are shown in Figure 6(c).

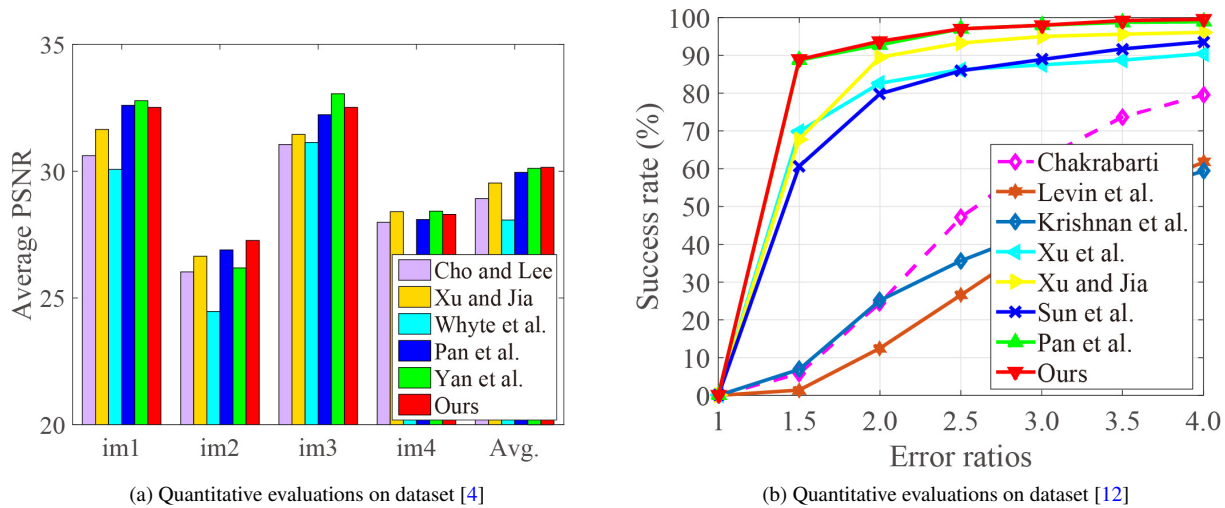
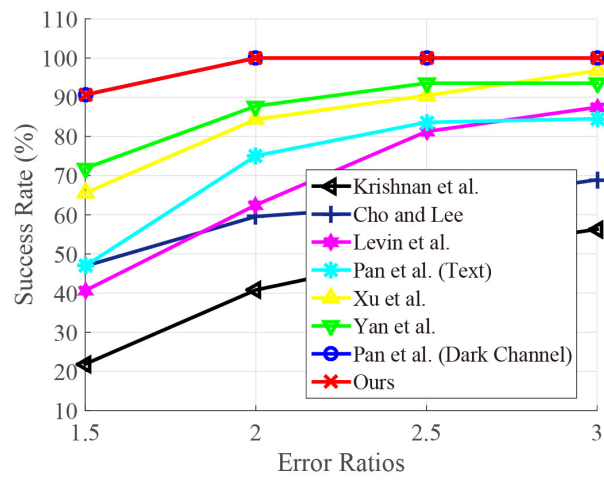


Figure 5. Quantitative evaluations on the benchmark datasets [4, 12]. The dataset by Köhler et al. [4] contains 48 blurred images, including 4 clear images and 12 challenging blur kernels. Our method generates results having the highest average PSNR among other state-of-the-art methods. The dataset by Sun et al. [12] contains 640 blurred images including 80 clear images and 8 blur kernels from [6]. Our method performs favorably against state-of-the-art methods.



(a) Comparisons with state-of-the-art methods



(b) Blurred images and the ground truth blur kernels



(c) Deblurred results by our method

Figure 6. Quantitative evaluations on the dataset by Levin et al. [6]. Our algorithm performs favorably against state-of-the-art methods. It achieves 90.60% at the error ratio 1.5 and 100% success rate at error ratio 2.

4. Additional Qualitative Comparisons

In this section, we provide more qualitative comparisons with state-of-the-art deblurring methods.

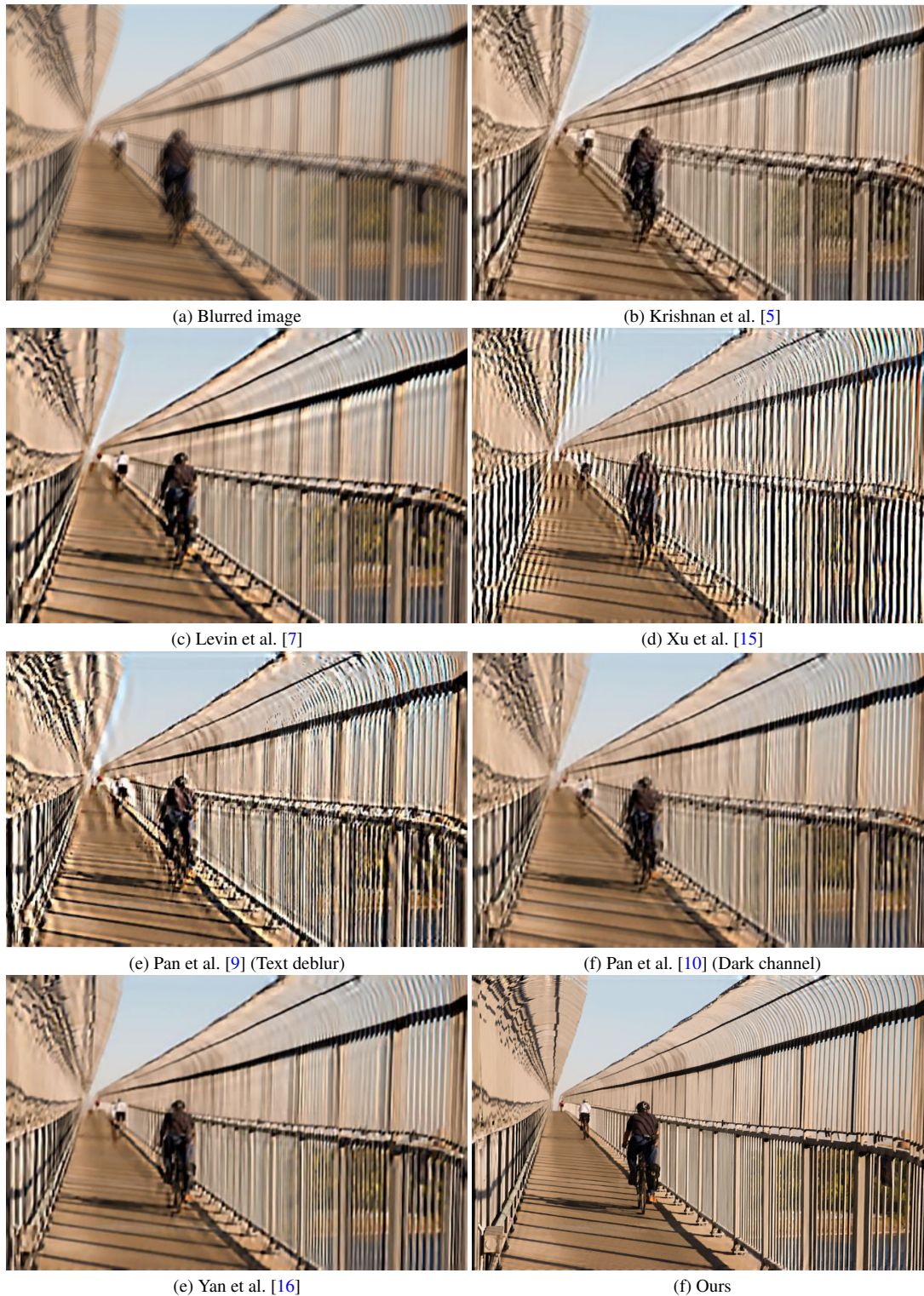


Figure 7. Comparisons with state-of-the-art deblurring methods on one blurred image reported from Yan et al. [16]. Our method generates better deblurring results.

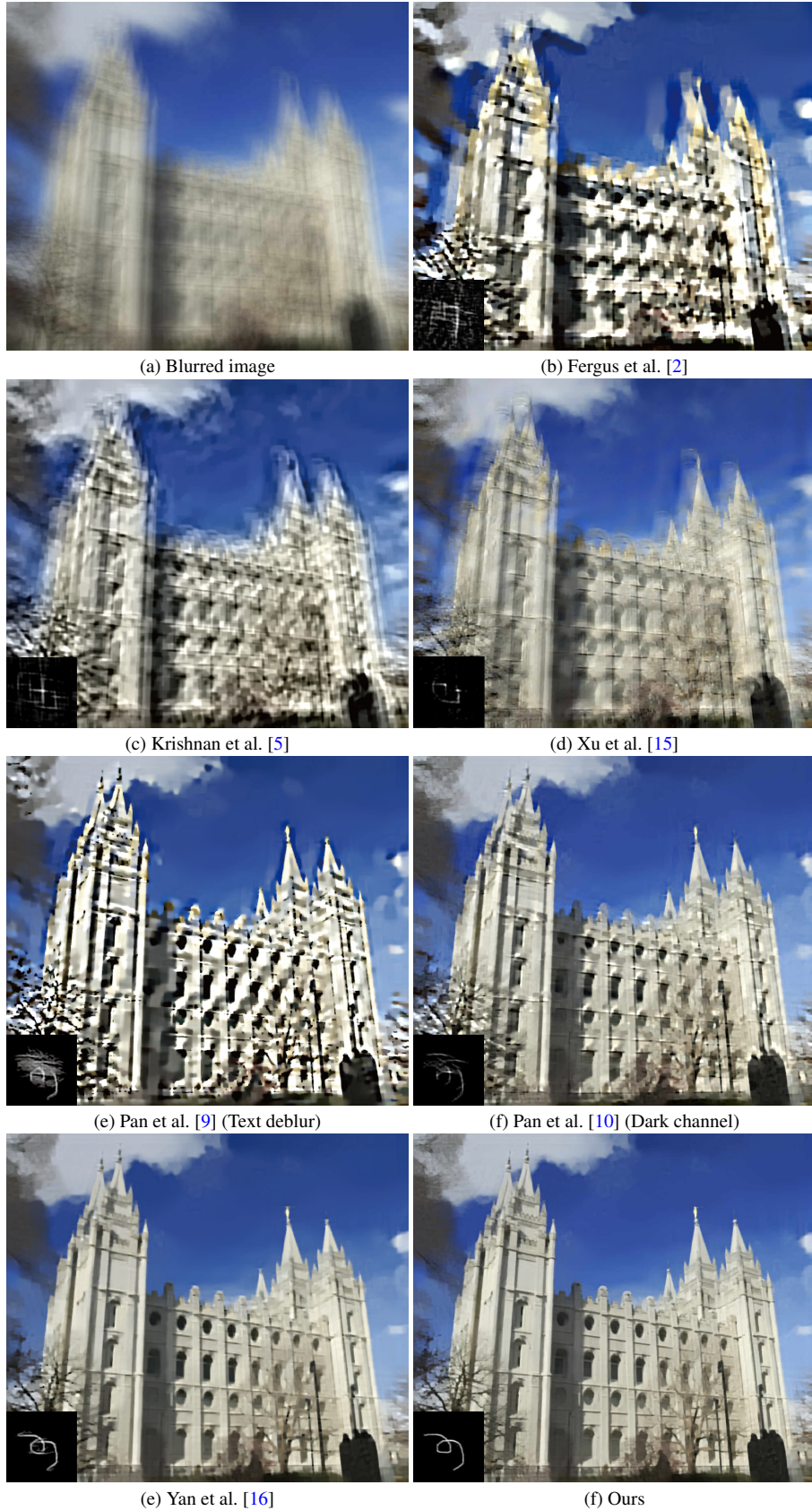


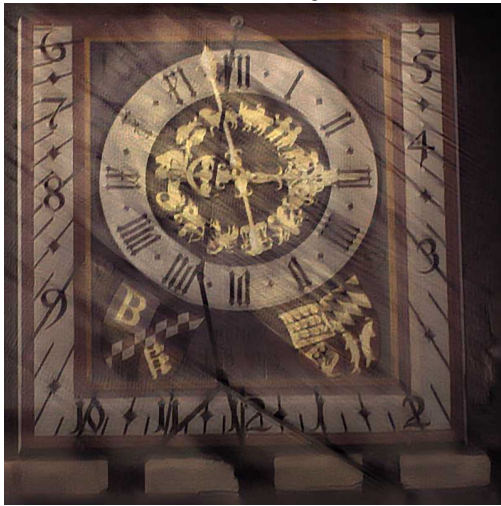
Figure 8. Comparisons with state-of-the-art deblurring methods on one blurred image using their provided codes. Our method generates better deblurring results.



(a) Blurred image



(b) Krishnan et al. [5]



(c) Shan et al. [11]



(d) Pan et al. [10]



(b) Yan et al. [16]



(c) Ours

Figure 9. A challenging example from dataset by Köhler et al. [4] and comparisons with state-of-the-art deblurring methods. Our method generates clearer images with less blur effect.

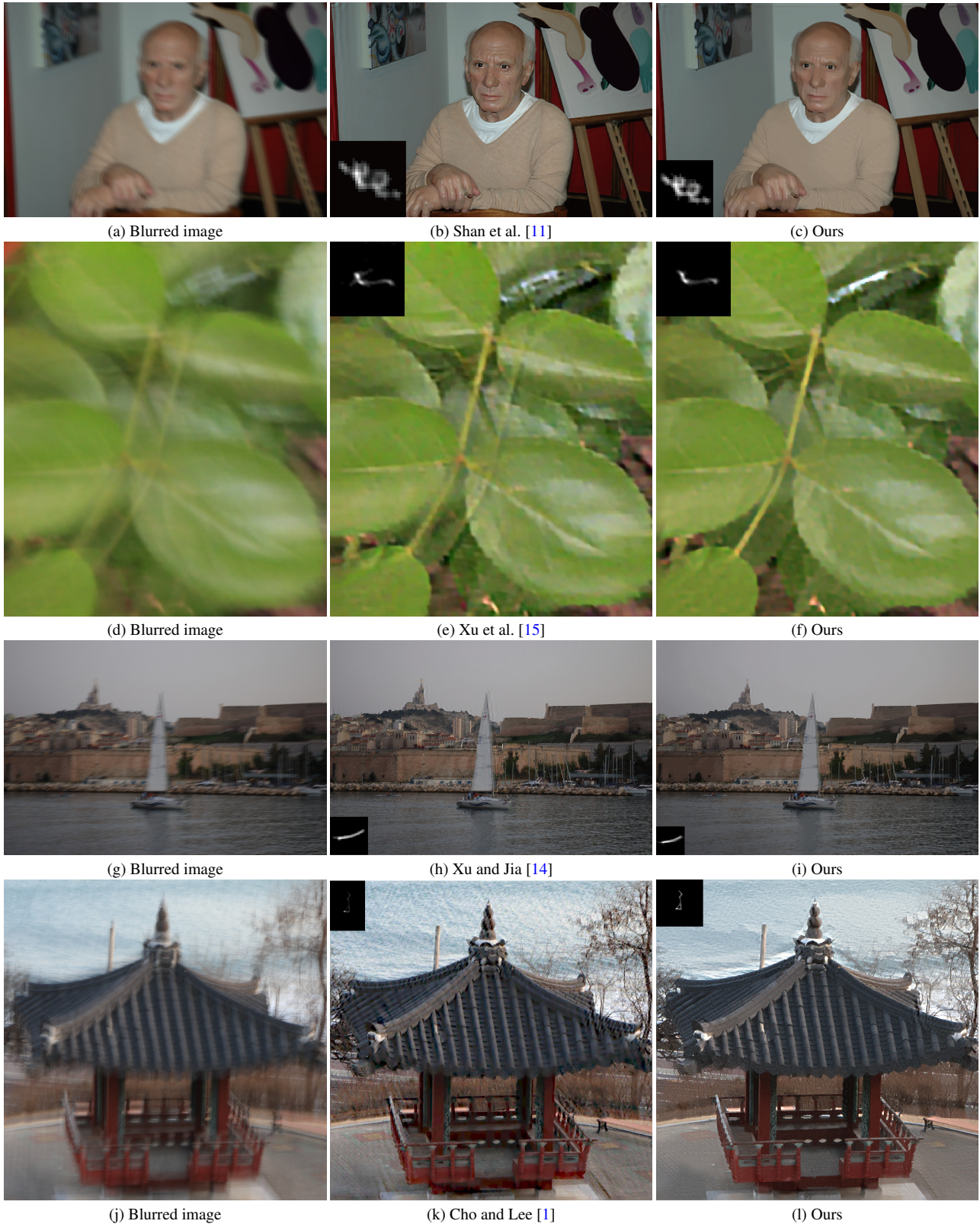


Figure 10. Comparisons with state-of-the-art deblurring methods using their provided examples and reported results. Our method generates visually comparable or even better deblurring results.

Motion and Tracking
Stereo and Structure from Motion
Shape-from-X
Color and Texture
Segmentation and Grouping
Image-Based Modeling
Illumination and Reflectance
Mobile vision
Shape Representation and Matching
Sensors
Early and Biologically-Inspired Vision
Computational Photography
Video

(a) Blurred image

Motion and Tracking
Stereo and Structure from Motion
Shape-from-X
Color and Texture
Segmentation and Grouping
Image-Based Modeling
Illumination and Reflectance
Mobile vision
Shape Representation and Matching
Sensors
Early and Biologically-Inspired Vision
Computational Photography
Video

(d) Pan et al. [10] (Dark Channel)

Motion and Tracking
Stereo and Structure from Motion
Shape-from-X
Color and Texture
Segmentation and Grouping
Image-Based Modeling
Illumination and Reflectance
Mobile vision
Shape Representation and Matching
Sensors
Early and Biologically-Inspired Vision
Computational Photography
Video

(b) Xu et al. [15]

Motion and Tracking
Stereo and Structure from Motion
Shape-from-X
Color and Texture
Segmentation and Grouping
Image-Based Modeling
Illumination and Reflectance
Mobile vision
Shape Representation and Matching
Sensors
Early and Biologically-Inspired Vision
Computational Photography
Video

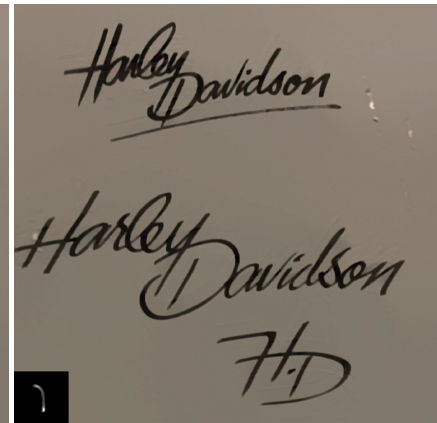
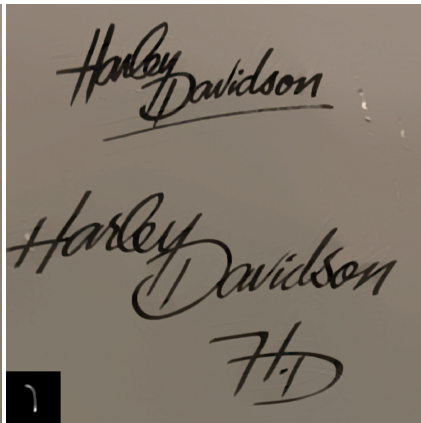
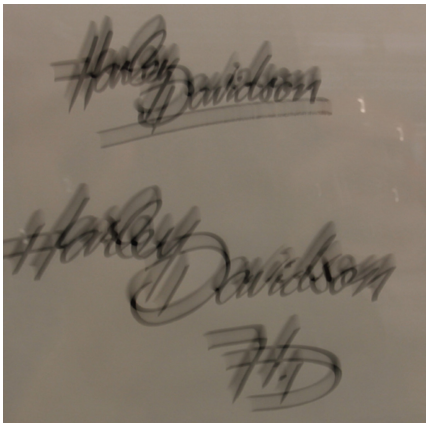
(e) Yan et al. [16]

Motion and Tracking
Stereo and Structure from Motion
Shape-from-X
Color and Texture
Segmentation and Grouping
Image-Based Modeling
Illumination and Reflectance
Mobile vision
Shape Representation and Matching
Sensors
Early and Biologically-Inspired Vision
Computational Photography
Video

(c) Pan et al. [9] (Text Deblurring)

Motion and Tracking
Stereo and Structure from Motion
Shape-from-X
Color and Texture
Segmentation and Grouping
Image-Based Modeling
Illumination and Reflectance
Mobile vision
Shape Representation and Matching
Sensors
Early and Biologically-Inspired Vision
Computational Photography
Video

(f) Ours



(g) Blurred image

(h) Pan et al. [9] (Text Deblurring)

(i) Ours

Figure 11. Comparisons with state-of-the-art methods on text blurred images. Our method generates better results than natural deblurring method [15, 10, 16] and performs favorably against the specially designed text deblurring method [9].

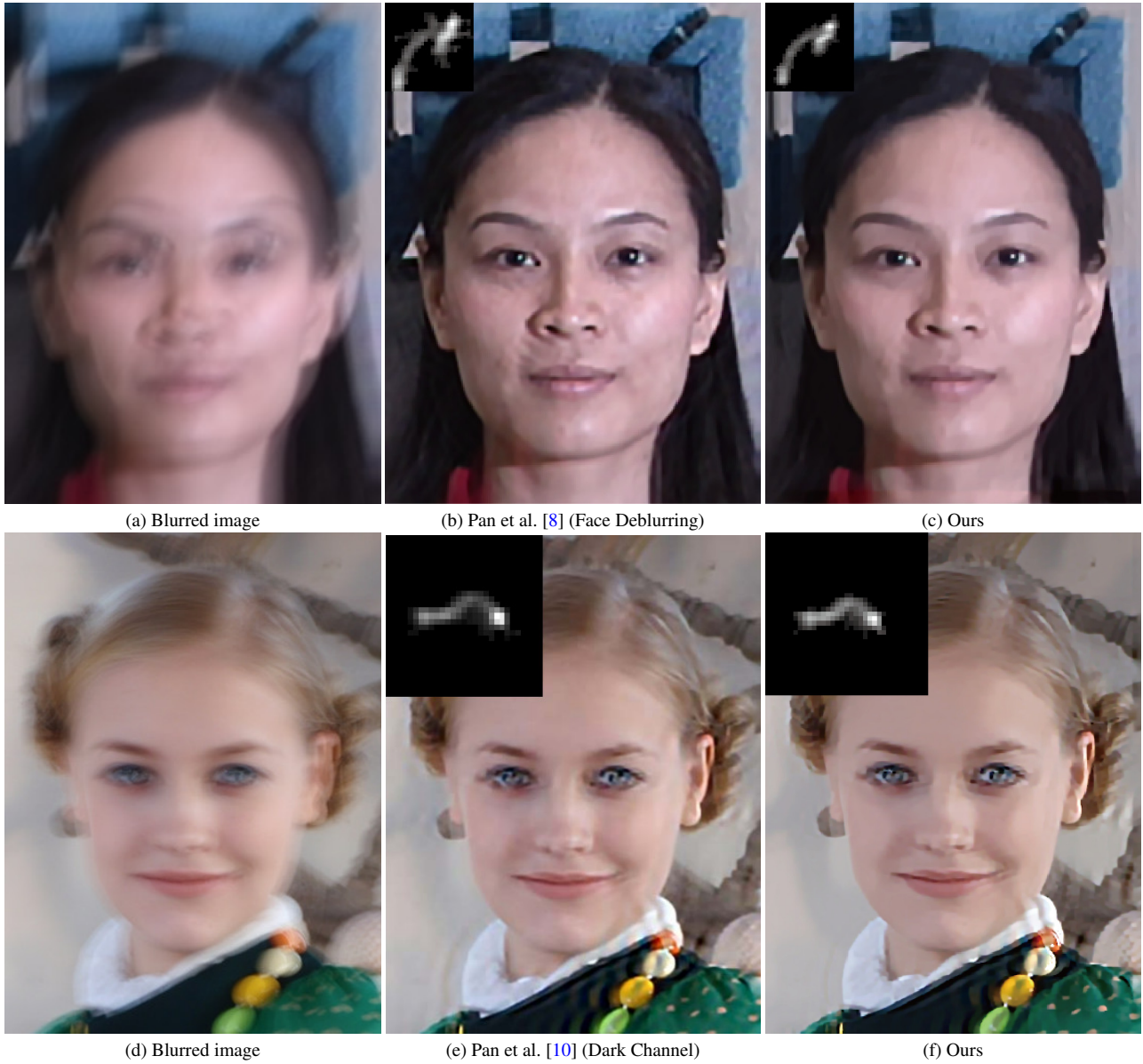
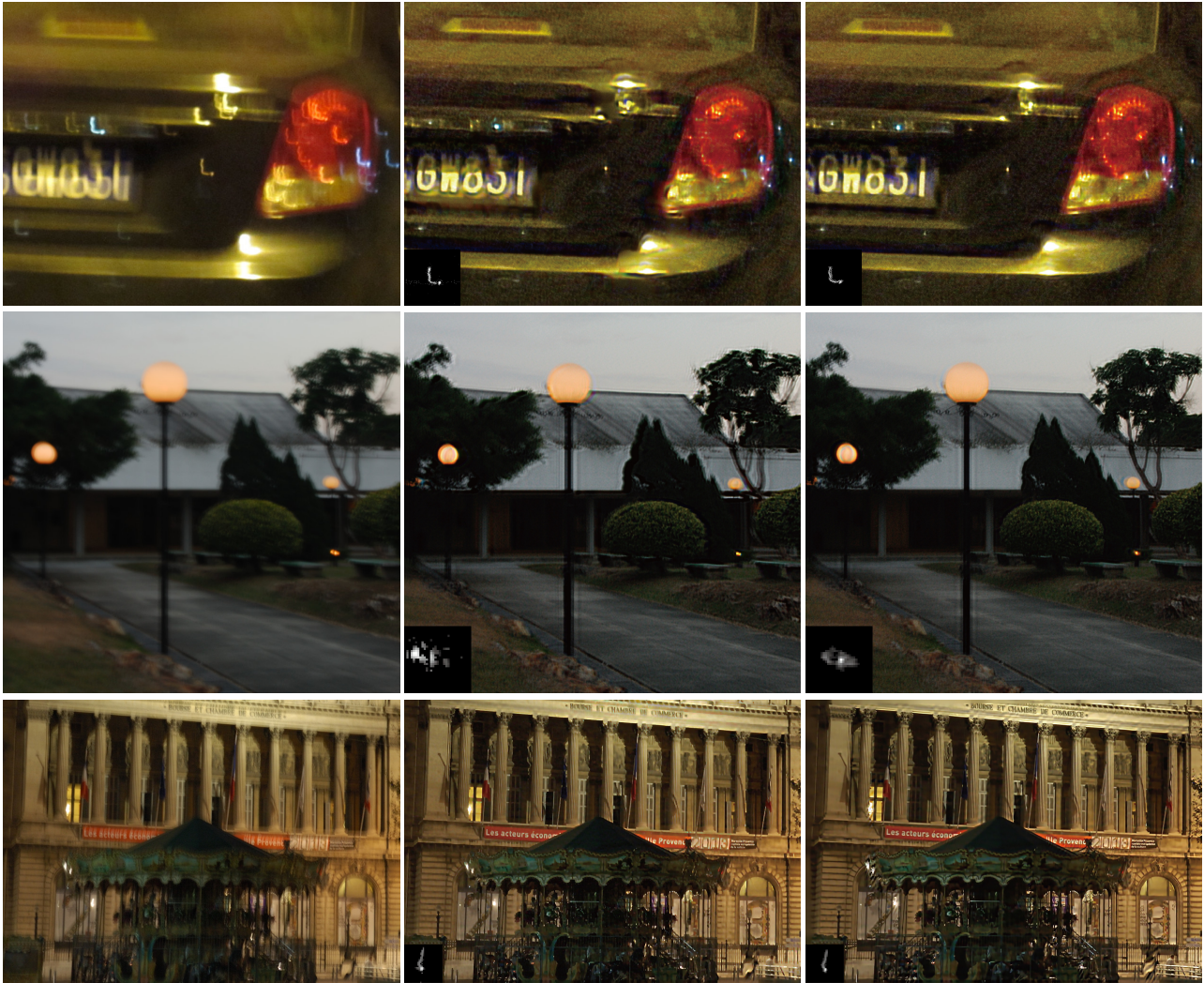


Figure 12. Comparisons with state-of-the-art methods on face blurred images. Our method generates comparable or even better deblurring results than state-of-the-art methods [8, 10].



(a) Blurred image

(b) Hu et al. [3]

(c) Ours

Figure 13. Comparisons with state-of-the-art methods on blurred images in low-illumination conditions. Our method generates comparable or even better results than method by Hu et al. [3].



(a) Blurred



(b) Whyte et al. [13]



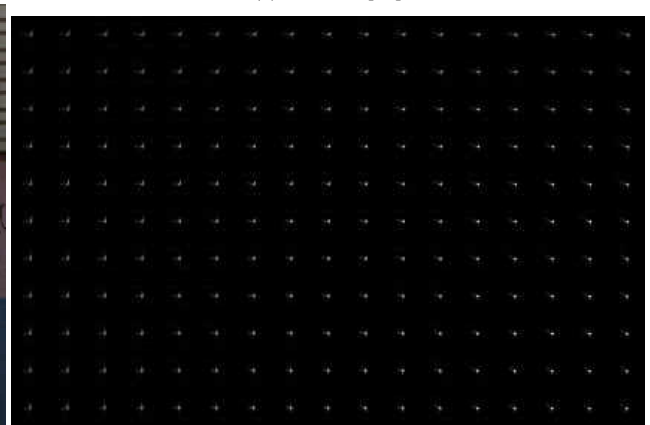
(c) Xu et al. [15]



(d) Pan et al. [10]



(e) Ours



(d) Our kernels

Figure 14. Deblurred results on a non-uniform blurred image. Our method provides comparable results with state-of-the-art methods.

References

- [1] S. Cho and S. Lee. Fast motion deblurring. *ACM Transactions on Graphics*, 28(5):145, 2009. 9
- [2] R. Fergus, B. Singh, A. Hertzmann, S. T. Roweis, and W. T. Freeman. Removing camera shake from a single photograph. *ACM Transactions on Graphics*, 25(3):787–794, 2006. 7
- [3] Z. Hu, S. Cho, J. Wang, and M.-H. Yang. Deblurring low-light images with light streaks. In *IEEE Conference on Computer Vision and Pattern Recognition*, 2014. 12
- [4] R. Köhler, M. Hirsch, B. Mohler, B. Schölkopf, and S. Harmeling. Recording and playback of camera shake: Benchmarking blind deconvolution with a real-world database. In *European Conference on Computer Vision*, 2012. 1, 4, 8
- [5] D. Krishnan, T. Tay, and R. Fergus. Blind deconvolution using a normalized sparsity measure. In *IEEE Conference on Computer Vision and Pattern Recognition*, 2011. 6, 7, 8
- [6] A. Levin, Y. Weiss, F. Durand, and W. T. Freeman. Understanding and evaluating blind deconvolution algorithms. In *IEEE Conference on Computer Vision and Pattern Recognition*, 2009. 1, 4, 5
- [7] A. Levin, Y. Weiss, F. Durand, and W. T. Freeman. Efficient marginal likelihood optimization in blind deconvolution. In *IEEE Conference on Computer Vision and Pattern Recognition*, 2011. 6
- [8] J. Pan, Z. Hu, Z. Su, and M.-H. Yang. Deblurring face images with exemplars. In *European Conference on Computer Vision*, 2014. 11
- [9] J. Pan, Z. Hu, Z. Su, and M. H. Yang. Deblurring text images via l0-regularized intensity and gradient prior. In *IEEE Conference on Computer Vision and Pattern Recognition*, 2014. 6, 7, 10
- [10] J. Pan, D. Sun, H. Pfister, and M.-H. Yang. Blind image deblurring using dark channel prior. In *IEEE Conference on Computer Vision and Pattern Recognition*, 2016. 2, 3, 4, 6, 7, 8, 10, 11, 13
- [11] Q. Shan, J. Jia, and A. Agarwala. High-quality motion deblurring from a single image. In *ACM Transactions on Graphics*, volume 27, page 73, 2008. 8, 9
- [12] L. Sun, S. Cho, J. Wang, and J. Hays. Edge-based blur kernel estimation using patch priors. In *IEEE International Conference on Computational Photography*, 2013. 1, 4
- [13] O. Whyte, J. Sivic, A. Zisserman, and J. Ponce. Non-uniform deblurring for shaken images. *International Journal of Computer Vision*, 98(2):168–186, 2012. 13
- [14] L. Xu and J. Jia. Two-phase kernel estimation for robust motion deblurring. In *European Conference on Computer Vision*, 2010. 9
- [15] L. Xu, S. Zheng, and J. Jia. Unnatural l0 sparse representation for natural image deblurring. In *IEEE Conference on Computer Vision and Pattern Recognition*, 2013. 6, 7, 9, 10, 13
- [16] Y. Yan, W. Ren, Y. Guo, R. Wang, and X. Cao. Image deblurring via extreme channels prior. In *IEEE Conference on Computer Vision and Pattern Recognition*, 2017. 2, 3, 4, 6, 7, 8, 10
- [17] D. Zoran and Y. Weiss. From learning models of natural image patches to whole image restoration. In *IEEE International Conference on Computer Vision*, 2011. 2